Appl. Phys. B (2015) 120:123–128
DOI 10.1007/s00340-015-6112-2

Applied Physics B
Lasers and Optics

Ho:KLuW microchip laser intracavity pumped by a diode-pumped Tm:KLuW laser

J. M. Serres[1] · P. A. Loiko[1,2] · X. Mateos[1] · K. V. Yumashev[2] · N. V. Kuleshov[2] · V. Petrov[3] · U. Griebner[3] · M. Aguiló[1] · F. Díaz[1]

Received: 3 December 2014 / Accepted: 11 April 2015 / Published online: 22 April 2015

Abstract A compact intracavity-pumped microchip Ho laser is realized using stacked Tm:KLuW/Ho:KLuW crystals pumped by a laser diode at 805 nm; both crystals are cut for light propagation along the N_g optical indicatrix axis and emit with polarization along the N_m axis. Maximum CW output power of 285 mW is achieved at a wavelength of 2080 nm for 5.6 W absorbed pump power in the Tm:KLuW crystal with a maximum slope efficiency of 8.3 %. Maximum total (Tm^{3+} and Ho^{3+} emission) output of 887 mW with a slope efficiency of 23 % is achieved. Laser operation is obtained in the 1867–1900 nm spectral range corresponding to the Tm emission, while Ho emits at 2078–2100 nm, depending on the output coupling. The microchip Ho laser generates a near-circular output beam with $M^2 < 1.1$. The compact laser setup with plane–plane cavity provides automatic mode-matching condition for the Tm and Ho laser modes.

1 Introduction

Holmium (Ho) lasers emitting slightly above 2 μm in the eye-safe spectral range are important for remote sensing, metrology and medical applications, as well as pumping of mid-IR optical parametric oscillators (OPOs). In the latter case, they are preferable compared to their thulium (Tm) counterparts emitting below 2 μm, because of the weaker residual absorption in the non-oxide nonlinear crystals employed in such OPOs [1]. Both Tm and Ho lasers exhibit a wide tunability range for laser emission on their ~2-μm transitions, around 200 nm at zero level, depending on the host.

Since Ho^{3+} ions do not absorb in the emission range of powerful laser diodes, sensitizing with Tm^{3+} is a common approach leading to strong absorption at ~800 nm ($^3H_6 \rightarrow {}^3H_4$ transition) suitable for pumping with commercial AlGaAs diodes [2]. The energy transfer takes place between the $^3F_4$ state of Tm and the $^5I_7$ state (upper-laser level) of Ho. This scheme suffers from the heat release related to up-conversion processes and the finite efficiency of the energy transfer. Thus, power scaling capability and achievable slope efficiency are limited. An alternative approach is the so-called resonant (inband) pumping of the Ho laser by bulk or fiber Tm lasers [3, 4]. In this case, the low quantum defect helps to suppress detrimental thermal effects and achieve high slope efficiency in room temperature operation. Such a scheme enables independent optimization of both lasers, including host selection and doping levels. A very similar approach is the so-called intracavity resonant pumping [5]. It enables a more compact design and mode matching of the Tm and Ho laser modes.

The concept of intracavity-pumped Ho lasers was proposed in [5] for Ho:YAG. The pump source was a Tm:YAG laser pumped in turn by a continuous-wave (CW) Ti:Sapphire laser. Both crystals were stacked together and placed in a common two-mirror cavity. The maximum output power was 125 mW in the CW regime at 2090 nm with a slope efficiency of 42 % (with respect to the absorbed

✉ X. Mateos
xavier.mateos@urv.cat

1 Física i Cristal·lografia de Materials i Nanomaterials (FiCMA-FiCNA), Universitat Rovira i Virgili (URV), Campus Sescelades, c/Marcel·lí Domingo, s/n., 43007 Tarragona, Spain

2 Center for Optical Materials and Technologies, Belarusian National Technical University, 65/17 Nezavisimosti Ave., 220013 Minsk, Belarus

3 Max Born Institute for Nonlinear Optics and Short Pulse Spectroscopy, 2A Max-Born-Str., 12489 Berlin, Germany

Ti:Sapphire laser power). Using a diode-pumped Tm:YAG laser, 2.1 W of CW output at 2097 nm were obtained from Ho:YAG in [6], with a slope of 25 % with respect to the incident diode power but relatively low beam quality (M^2 = 1.6). Later on, with a similar setup, these results were improved in terms of output power up to 7.2 W, albeit at reduced slope efficiency, 17.5 %, as well as strongly non-Gaussian beam profile, M^2 ~ 6 [7]. A theoretical analysis of such lasers was presented in [8].

In [9], an Ho:YAG crystal was placed inside the cavity of a Tm:YLF diode-pumped laser; however, it had its own cavity and was transversally pumped. With such a special design, 14 W of CW Ho emission at 2.09 μm was obtained with a slope efficiency of 16 %. A typical coupled cavity approach was used in [10] for a Ho:YAG intracavity pumped by a Tm:YLF diode-pumped laser. In this case, pulsed laser operation was detected for both Tm and Ho lasers, with typical pulse durations of 2–3 μs and 200 ns, respectively, and maximum average output of 1.6 W at 2090 nm with a slope efficiency of ~21 %. This temporal behavior was explained by the fact that Ho:YAG can act as a saturable absorber to Q-switch the Tm laser [11], with subsequent gain-switching effect on the Ho laser.

In this study, we present the first realization of a CW intracavity inband-pumped microchip Ho laser with a nearly perfect beam quality, M^2 < 1.1. To this aim, we employed a monoclinic potassium lutetium double tungstate crystal, $KLu(WO_4)_2$ or shortly KLuW, doped with Ho^{3+} ions. For intracavity pumping, a similar Tm:KLuW crystal was used. The selection of a monoclinic double tungstate as a laser host is due to their beneficial spectroscopic properties, namely wide and intense absorption and emission bands, as well as high achievable doping levels [12]. The possibility of microchip operation is due to a special crystal cut, as shown recently for Tm-doped monoclinic double tungstates [13–15].

2 Experimental

The Ho crystal used in the present study was a 3 at.% Ho:KLuW grown by the top-seeded solution growth (TSSG) slow-cooling method using a seed with its *b*-axis oriented perpendicular to the solution [16]. The actual Ho ion density measured by electron probe microanalysis (EPMA) was 2.54 × 10^{20} at/cm^3. For the as-grown crystal, a rectangular sample with dimensions 2.67(N_g) × 2.95(N_m) × 3.04(N_p) mm^3 along the indicated (orthogonal) optical indicatrix axes. This sample was oriented for light propagation along the N_g axis (further N_g cut), and the input and output m × p crystal faces were polished to laser quality and antireflection (AR) coated for the range of 1820–2075 nm. For intracavity pumping, we employed an uncoated 3 at.% Tm:KLuW crystal (N_{Tm} = 2.15 × 10^{20} at/cm^3) cut along the N_g axis (2.33 mm thick) with an aperture of 2.95(N_m) × 3.01(N_p) mm^2. Both crystals were mounted in single copper holder water-cooled to 14 °C. Indium foil was used to improve the thermal contact between crystals and cooling holder. The m × p faces of the two crystals were in contact with identical orientation of the N_m and N_p principal optical axes.

The pump mirror (PM) of the microchip laser cavity was flat; it was AR coated for 770–1050 nm, and high reflection (HR, R > 99.9 %) coated for 1820–2075 nm. It was attached directly to the back face of the crystal stack. A flat output coupler (OC) had a nominal transmittance, T_{OC} = 0.2, 1.5, 3 or 5 %, for the range 1820–2075 nm. For the actual transmittances of the OCs at laser wavelengths, please refer to Table 1. The air gap between the output face of the crystal stack and OC was <200 μm. The Tm:KLuW crystal was pumped with a fiber-coupled (NA = 0.22, fiber core diameter: 200 μm) laser diode emitting at ~805 nm with a maximum output power of 25 W. The output of the diode was reimaged into the crystal by a lens assembly with 1:1 imaging ratio. Thus, the pump spot radius in the crystal amounted to 100 μm. The total average absorption of the unpolarized pump in the Tm:KLuW crystal was 59 %, no absorption saturation or any dependence on the pump level was observed.

Table 1 Wavelengths of the Tm and Ho emissions from the intracavity-pumped Ho:KLuW microchip laser (λ_{Tm} and λ_{Ho}) and actual transmittances of output couplers, T_{OC}, at the laser wavelengths

Nominal T_{OC} (%)	λ_{Ho}, nm	Actual T_{OC} (%)	λ_{Tm}, nm	Actual T_{OC} (%)
0.2	2095/2100	0.4	1888	<0.05
1.5	2081	2.1	1877–1900	1.5
3	2080	3.3	1867–1900	2.8
5	2078	5.4	1873–1900	5.0

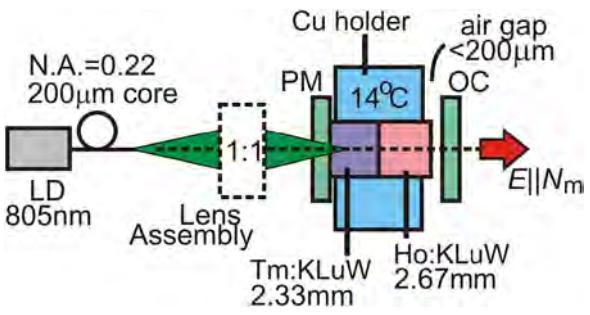

Fig. 1 Scheme of the Ho:KLuW microchip laser intracavity pumped by a diode-pumped Tm:KLuW laser; *PM* pump mirror, *OC* output coupler, *LD* laser diode

The scheme of intracavity-pumped Ho:KLuW laser is shown in Fig. 1. According to previous studies [17, 18], the main feature of a microchip setup is a plano–plano laser cavity with at least one mirror attached to the gain medium (for instance, even directly coated on its face). If there are no air gaps in the setup and both PM and OC are directly coated on the crystal, a monolithic microchip setup is produced. In our case, we can talk about quasi-monolithic microchip setup that is eligible for the demonstration of future prospects of such kind of lasers.

3 Results and discussion

Ho laser operation was obtained for all studied T_{OC}. Tm emission as a precondition for the Ho emission was also detected. The laser output for both ions was linearly polarized, along the N_m axis. In order to separate the contributions from Tm and Ho emission, we used a special dichroic mirror. The corresponding input–output curves are shown in Fig. 2 with respect to the absorbed diode laser pump power in the Tm:KLuW crystal. Here, circles and triangles correspond to Ho and Tm laser contributions, squares represent total output, and lines represent the slope fitting. The output characteristics of the intracavity-pumped Ho:KLuW microchip laser are also summarized in Table 2.

The total output of the laser P_Σ and the total slope efficiency η_Σ increase with T_{OC}. Maximum $P_\Sigma = 887$ mW is obtained for $T_{OC} = 5$ %; the corresponding maximum η_Σ value is 23.3 %; the absorbed pump power is 5.1 W; and the optical-to-optical efficiency is 18 %. The laser threshold in this case is at 1.1 W. The total input–output dependences are clearly linear; no detrimental influence of thermal effects is observed even for high pump levels.

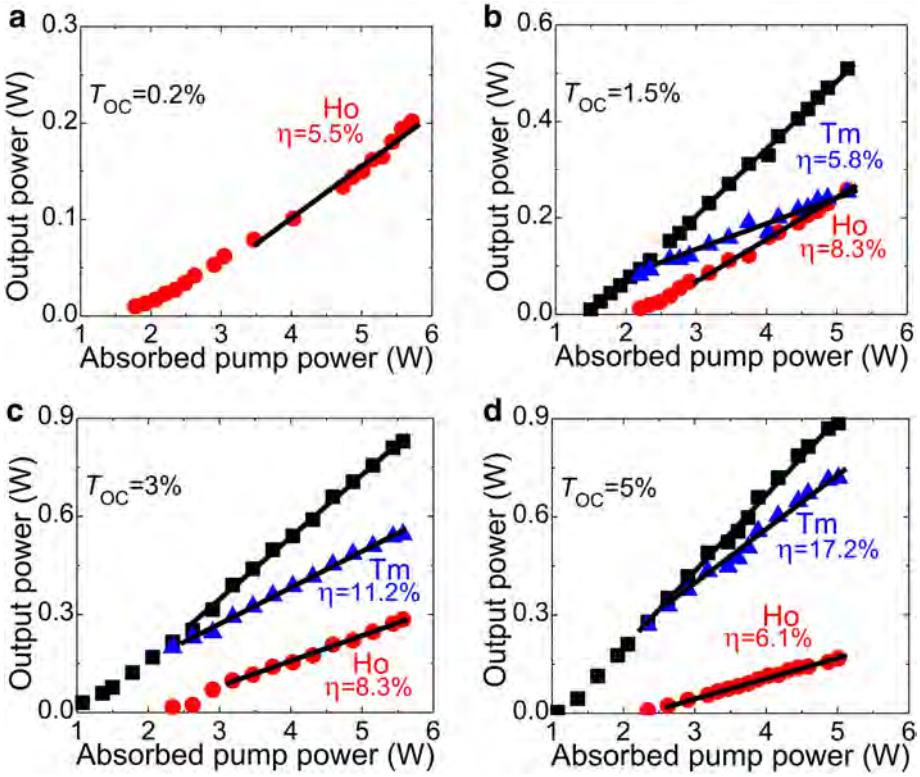

Fig. 2 Input–output curves of the Ho:KLuW microchip laser intracavity pumped by a Tm:KLuW laser: *Squares* represent the total output, *circles* and *triangles* correspond to the Ho and Tm emission, respectively, **a–d** plots correspond to $T_{OC} = 0.2$, 1.5, 3 and 5 %, respectively

Table 2 Output characteristics[a] of the intracavity-pumped Ho:KLuW microchip laser, intracavity pumped by a Tm:KLuW laser

T_{OC} (%)	η_Σ (%)	P_Σ, mW	η_{Ho} (%)	η_{Ho}/η_Σ	P_{Ho}, mW	P_{th}, W
0.2	5.5	202	5.5	0.99	202	1.7
1.5	14.1	510	8.3	0.59	257	2.1
3	19.4	782	8.3	0.43	285	2.3
5	23.3	887	6.1	0.26	168	2.4

[a] η_Σ and η_{Ho} are the slope efficiencies for total output and Ho emission; P_{Ho} and P_{th} are the maximum output power and the threshold for Ho laser; P_Σ is the maximum total output power of the Tm:KLuW and Ho:KLuW laser

The maximum Ho laser output P_{Ho} of 285 mW and the maximum slope efficiency η_{Ho} of 8.3 % are achieved for $T_{OC} = 3$ %, the optimal T_{OC} for Ho laser operation. This corresponds to 5.6 W of absorbed diode laser power and 5 % optical-to-optical efficiency. The Ho laser threshold is 2.3 W. For lower and higher output coupling, reduction in both P_{Ho} and η_{Ho} is observed.

The ratio of the slopes of Ho and Tm emissions, showing the efficiency of the intracavity pumping, is maximum for $T_{OC} = 0.2$ %. In this case, the Tm laser output power is <1 % of the total power, thus η_{Ho}/η_{Σ} ~0.99. With the increase in T_{OC}, this ratio continuously decreases, and it equals only η_{Ho}/η_{Σ} ~0.26 for $T_{OC} = 5$ %. As expected, the threshold of the Ho laser increases with output coupling, from 1.7 W for $T_{OC} = 0.2$ % to 2.4 W for $T_{OC} = 5$ % (again in terms of absorbed diode laser pump power in the Tm:KLuW crystal). The ratio η_{Ho}/η_{Σ} amounted to ~0.9 in the intracavity-pumped Ho:YAG laser described in [5]. Lower values are associated with the leakage of Tm power through the broadband OC (see Table 1). In our experiment, the difference in the OC transmission for the two lasers is significant only for the 0.2 % OC. Thus, much higher Ho laser efficiency and output power can be expected with dichroic mirrors, providing negligible output coupling for the Tm laser also at higher transmission for the Ho laser.

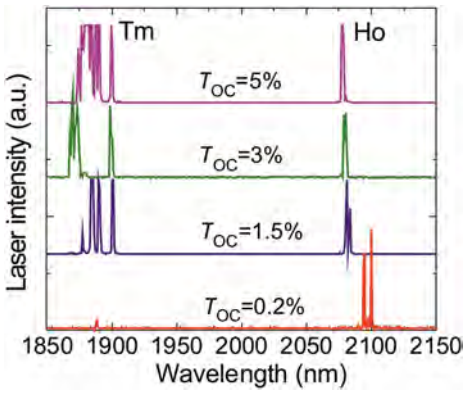

Fig. 3 Spectra of the emission from the Ho:KLuW microchip laser intracavity pumped by a Tm:KLuW laser for different T_{OC}

Spectra of laser emission of the intracavity-pumped Ho:KLuW microchip are shown in Fig. 3. Ho laser operation occurs at 2095/2100 nm (two peaks) for $T_{OC} = 0.2$ %. For higher output coupling, the wavelength of Ho emission is in the 2078–2081 nm range. This can be explained, considering the gain cross-sectional (σ_g) spectrum of Ho:KLuW for the laser polarization, $E\|N_m$, see Fig. 4a, absorption and stimulated-emission cross-sectional spectra of Ho:KLuW were taken from [16]. For low T_{OC} (and, hence, small inversion ratio β), laser oscillation up to 2100 nm is possible, while the increase in β (associated with higher T_{OC}) results in the formation of a local maximum in the gain spectrum, around 2079 nm. For a further increase of β laser operation at ~2058 nm is also expected.

Thulium laser operation is observed in the range of 1867–1900 nm for all OCs. It is shorter than the laser wavelength of the Tm:KLuW microchip laser described in [14], ~1946 nm. We attribute this to the increased losses for Tm emission associated with the absorption by the Ho:KLuW crystal. Also, this is consistent with the gain cross-sectional spectrum of Tm:KLuW [12] for laser polarization, $\boldsymbol{E}\|N_m$, and high β, see Fig. 4b. Table 1 summarizes the Tm and Ho laser wavelengths as well as the actual values of T_{OC} at these lines.

Thus, intracavity pumping of the Ho:KLuW crystal mainly takes place into the short-wavelength tail of the absorption band corresponding to the $^5I_8 \rightarrow {}^5I_7$ transition, see Fig. 4c with a black rectangle representing the wavelengths from Tm emission. Although the absorption of Ho:KLuW at such wavelengths, which plays the role of a loss, is higher for $E\|N_m$ (σ_{abs} ~ 0.2 × 10^{-20} cm^2) compared to $E\|N_p$ (σ_{abs} ~ 0.05 × 10^{-20} cm^2), see Fig. 4c, the Tm:KLuW laser still oscillates with $E\|N_m$. This is due to a significant anisotropy of gain cross sections in Tm:KLuW

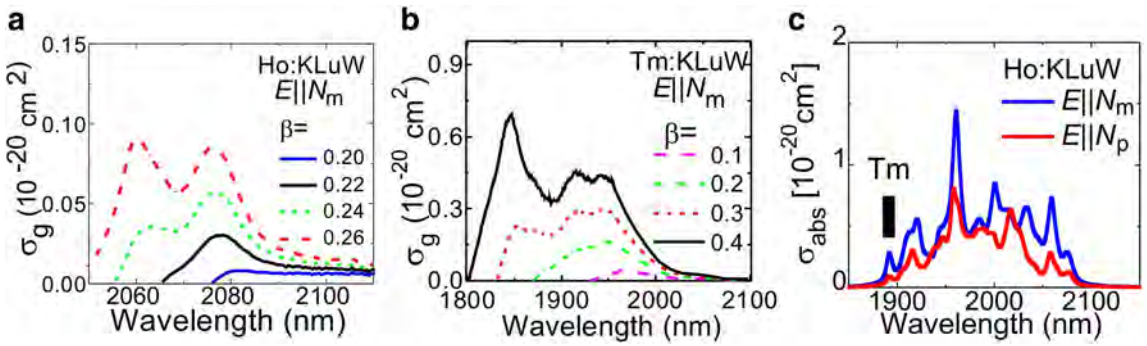

Fig. 4 Gain cross-sectional σ_g spectra of Ho:KLuW (**a**) and Tm:KLuW (**b**) crystals for light polarization $\boldsymbol{E}\|N_m$; anisotropy of the absorption band corresponding to the $^5I_8 \rightarrow {}^5I_7$ transition of Ho:KLuW (**c**); *black rectangle* in (**c**) part represents the wavelengths of Tm laser emission

for large inversion ratios ($\beta \sim 0.4$), with $\sigma_g(m)$ being at least two times higher than $\sigma_g(p)$. As for the absolute value, $\sigma_g(m)$ ~0.5×10^{-20} cm^2 for the above-mentioned wavelengths exceeds the losses due to the absorption in Ho:KLuW crystal. Note that in an anisotropic material such as KLuW, absorption losses in an intracavity-pumped laser may in principle lead not only to wavelength shifts as discussed for the YAG laser in [5] but also to polarization switching of the Tm laser [19].

The stabilization of the resonator mode in the intracavity-pumped Ho:KLuW microchip laser is provided by a positive thermal lens induced in the diode-pumped N_g-cut Tm:KLuW crystal. For the pump spot radius $w_p = 100$ μm, the sensitivity factor $M = dD/dP_{abs}$ was determined to be +12.9 m^{-1}/W [20]. The contribution of the lens in the Ho:KLuW crystal (which is also positive) is weak. Indeed, in the latter case, the fractional heat loading is determined as quantum defect, $\eta_h = 1 - \lambda_{Tm}/\lambda_{Ho} = 0.1 \pm 0.02$ in our case, compared with $\eta_h = 0.25 \pm 0.05$ [21] for Tm:KLuW. The latter value is related to the efficient two-for-one cross-relaxation scheme for Tm^{3+} ions that reduces the heat loading. Also, the absorbed pump power for the Ho:KLuW crystal is much lower. Finally, the so-called thermal mechanism of mode stabilization is observed. The calculated radii of the laser mode for Tm and Ho emission are 70 ± 5 μm (for "hot" cavity). The intracavity pumping scheme automatically produces optimal mode matching for Tm and Ho laser modes.

The studied microchip laser generates a near-circular output beam. To illustrate this, we captured the spatial profile of the Ho laser mode at 15 cm from the OC (for $T_{OC} = 3$ % and $P_{abs} = 5$ W), see Fig. 5a. In addition to the 2D plot, the intensity distributions along N_m and N_p directions, as well as Gaussian fits, are shown (the goodness of fits $R^2 > 0.98$). For this measurement, a FLIR SC7210 thermal imaging camera was used. To measure M^2 factors of the Ho laser mode, we used an ISO standard method [22], with a focusing ($f = 5$ cm) lens positioned at 10 cm from the OC, see Fig. 5b. The beam radii were measured with the optical knife method [22]. The M^2 factors along N_m and N_p directions are both below 1.1. Very similar beam characteristics were also detected for Tm laser mode; this is due to the automatic mode matching, as mentioned above.

Thus, an improvement of the quality of the output beam is achieved, as compared with the previous Ho intracavity-pumped lasers [6–10] although isotropic or uniaxial crystals were employed in these works. We attribute this progress partially to the simple laser setup with a common cavity for the Tm and Ho lasers and the longitudinal pumping. Even more important is that the chosen cut of the Tm:KLuW crystal, along the N_g axis, possesses a relatively weak and low-astigmatic thermal lens. It is even weaker compared to Tm:YAG. Indeed, the "generalized" thermo-optic coefficient χ that determines the optical power of the thermal lens, equals $\chi_{Tm:YAG}$ ~16×10^{-6} K^{-1} [23] and $\chi_{Tm:KLuW} = 8.8 \times 10^{-6}$ K^{-1} [14]. Finally, this moderated thermal lens effects lead to low distortions in the spatial profile of the output beam in our case.

Recently, we studied Ho:KLuW microchip lasers also with the two standard schemes of pumping of Ho^{3+} ions. In [24], a co-doped Tm, Ho crystal was pumped by a commercial AlGaAs diode at 805 nm, and 450 mW of CW output was extracted at 2081 nm with a slope efficiency of 31 % with respect to the absorbed diode power. Strong up-conversion in the Tm^{3+}-Ho^{3+} system was recognized to be a limitation for further power scaling of Ho output due to a significant heat loading. Later in [25], we studied singly doped Ho:KLuW microchip laser inband pumped

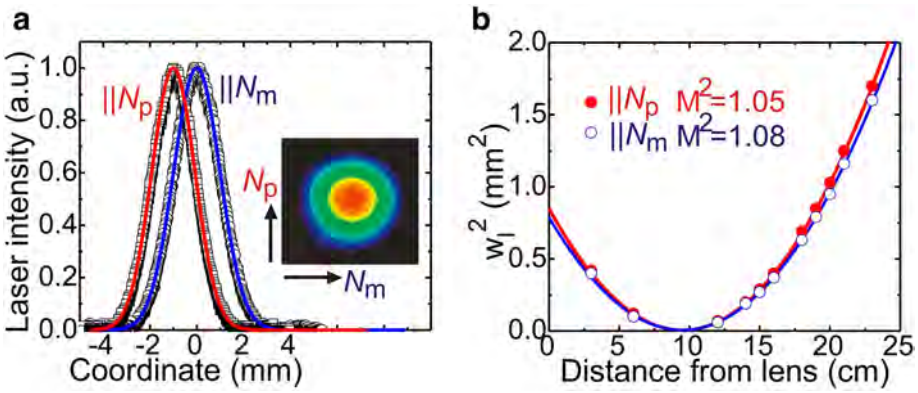

Fig. 5 **a** Intensity distributions along N_m and N_p directions for Ho laser mode of Ho:KLuW microchip laser (*symbols*—experimental data, *curves*—Gaussian fits, $R^2 > 0.98$), *inset* shows a spatial profile of the beam; as measured at 15 cm from the output coupler; $T_{OC} = 3$ % and $P_{abs} = 5$ W; **b** Evaluation of M^2 factors for N_m and N_p directions for Ho laser mode, w_l is the mode radius (*symbols*—experimental data, *curves*—parabolic fits)

by a Tm:KLuW laser. In that experiment, only 201 mW was achieved at 2105 nm with a record slope efficiency of 84 % with respect to the absorbed Tm laser power. However, the relatively low absorption in the Ho crystal due to imperfect matching of Tm laser wavelength with the absorption spectrum of Ho:KLuW limits its optical-to-optical efficiency to ~12 %. The scheme of pumping studied in the present paper presents an intermediate situation, as it is free of up-conversion losses and imply low heat load due to the use of inband pumping. It also utilizes a simple laser setup. However, in this scheme, it is difficult to reach high slope efficiencies as for "pure" inband pumping. In particular, the improvement of the slope efficiency and output power for the presented Ho:KLuW microchip will require reduction in the losses via AR coatings on the Tm:KLuW crystal, resulting in the shift of λ_{Tm} to longer wavelengths and, hence, higher absorption in the Ho:KLuW crystal, as well as optimization of the Tm/Ho doping ratio and the OC characteristics for minimum outcoupling of the Tm laser radiation and optimum outcoupling of the Ho laser.

4 Conclusions

A compact Ho:KLuW microchip laser intracavity inband pumped by a diode-pumped Tm:KLuW laser and operating at room temperature is realized, representing the first intracavity-pumped microchip Ho laser. The maximum CW output power of 285 mW is obtained at the wavelength of 2080 nm (Ho emission) for 5.6 W of absorbed diode laser power in the Tm:KLuW crystal with a maximum slope efficiency of 8.3 %. Maximum total (Tm^{3+} and Ho^{3+} emission) output of 887 mW with a slope efficiency of 23 % is achieved. Tm laser operation corresponds to the 1867–1900 nm spectral range, while Ho emits at 2078–2100 nm, depending on the output coupling. The positive thermal lens for the selected cut of the Tm:KLuW and Ho:KLuW crystals, along the N_g axis, ensures mode stabilization in the microchip cavity, as well as automatic mode-matching conditions for the Tm and Ho laser modes. The chosen geometry of both, the Tm:KLuW and the Ho:KLuW crystal cuts, is also responsible for the excellent quality of the laser beam.

References

1. P.A. Budni, L.A. Pomeranz, M.L. Lemons, C.A. Miller, J.R. Mosto, E.P. Chicklis, JOSA B **17**, 723 (2000)
2. T.Y. Fan, G. Huber, R.L. Byer, P. Mitzscherlich, Opt. Lett. **12**, 678 (1987)
3. D.Y. Shen, A. Abdolvand, L.J. Cooper, W.A. Clarkson, Appl. Phys. B **79**, 559 (2004)
4. P.A. Budni, M.L. Lemons, J.R. Mosto, E.P. Chicklis, IEEE J. Sel. Top. Quantum Electron. **6**, 629 (2000)
5. R.C. Stoneman, L. Esterowitz, Opt. Lett. **17**, 736 (1992)
6. C. Bollig, R.A. Hayward, W.A. Clarkson, D.C. Hanna, Opt. Lett. **23**, 1757 (1998)
7. R. A. Hayward, W. A. Clarkson, D. C. Hanna: in *Advanced Solid-State Lasers, Davos*, Switzerland, Technical Digest, paper MB8, 13–16 Feb 2000
8. M. Schellhorn, A. Hirth, IEEE J. Quantum Electron. **38**, 1455 (2002)
9. S. So, J.I. Mackenzie, D.P. Shepherd, W.A. Clarkson, J.G. Betterton, E.K. Gorton, J.A.C. Terry, Opt. Express **14**, 10481 (2006)
10. M. Schellhorn, A. Hirth, C. Kieleck, Opt. Lett. **28**, 1933 (2003)
11. Y.-K. Kuo, Y.-A. Chang, Appl. Opt. **42**, 1685 (2003)
12. V. Petrov, M.C. Pujol, X. Mateos, O. Silvestre, S. Rivier, M. Aguiló, R.M. Solé, J. Liu, U. Griebner, F. Díaz, Laser Photon. Rev. **1**, 179 (2007)
13. M.S. Gaponenko, P.A. Loiko, N.V. Gusakova, K.V. Yumashev, N.V. Kuleshov, A.A. Pavlyuk, Appl. Phys. B **108**, 603 (2012)
14. J.M. Serres, X. Mateos, P. Loiko, K. Yumashev, N. Kuleshov, V. Petrov, U. Griebner, M. Aguiló, F. Díaz, Opt. Lett. **39**, 4247 (2014)
15. M. Gaponenko, N. Kuleshov, T. Sudmeyer, Opt. Express **22**, 11578 (2014)
16. V. Jambunathan, X. Mateos, M.C. Pujol, J.J. Carvajal, C. Zaldo, U. Griebner, V. Petrov, M. Aguiló, F. Díaz, Appl. Phys. B **116**, 455 (2014)
17. J.J. Zayhowski, A. Mooradian, Opt. Lett. **14**, 24 (1989)
18. J.J. Zayhowski, C. Dill III, Opt. Lett. **19**, 1427 (1994)
19. M. Segura, X. Mateos, M.C. Pujol, J.J. Carvajal, M. Aguiló, F. Díaz, U. Griebner, V. Petrov, Appl. Phys. B **113**, 125 (2013)
20. P.A. Loiko, J.M. Serres, X. Mateos, K.V. Yumashev, N.V. Kuleshov, V. Petrov, U. Griebner, M. Aguiló, F. Díaz, Laser Phys. Lett. **11**, 075001 (2014)
21. P.A. Loiko, S.M. Vatnik, I.A. Vedin, A.A. Pavlyuk, K.V. Yumashev, N.V. Kuleshov, Laser Phys. Lett. **10**, 125005 (2013)
22. N. Hodgson, H. Weber, *Laser Resonators and Beam Propagation. Fundamentals, Advanced Concepts, Applications* (Springer, New York, 2005)
23. S. Chenais, F. Druon, S. Forget, F. Balembois, P. Georges, Progress. Quantum Electron. **30**, 89 (2006)
24. P. Loiko, J.M. Serres, X. Mateos, K. Yumashev, N. Kuleshov, V. Petrov, U. Griebner, M. Aguiló, F. Díaz, Opt. Express **22**, 27976 (2014)
25. P. Loiko, J.M. Serres, X. Mateos, K. Yumashev, N. Kuleshov, V. Petrov, U. Griebner, M. Aguiló, F. Díaz, Opt. Lett. **40**, 34 (2015)